Nonlinear inversion for stress- and fluid-sensitive parameters

Huaizhen Chen, Kristopher Innanen, Department of Geoscience, University of Calgary*

SUMMARY

Based on Gassmann's fluid substitution model, we set up a workflow for nonlinear inversion of seismic data for dry rock moduli, fluid factors and a stress-sensitive parameter. We first make an approximation within the fluid substitution equation, replacing the porosity term with a stress-sensitive parameter. We then derive a linearized reflection coefficient in terms of a stress-parameter reflectivity, and re-express it in terms of elastic impedance (EI). An amplitude-variation-with-offset (AVO) inversion workflow is set up, in which the seismic data are transformed to EI, after stacking within three incidence angle ranges; these are then inverted to determine the stress-sensitive parameter. The two-step process involves two inversions with significantly different properties. The first is a model-based least-squares inversion (in the estimation of EI); the second is a more complex nonlinear inversion of the EI for a set of unknowns including the stress parameter. Motivated by an interest in hybridizing AVO and full waveform inversion (FWI), we set the latter step up to resemble some features of a published AVO-FWI formulation. The approach is subjected to synthetic validation, which permits us to analyze the response and test the stability of the workflow. The response of the workflow to data acquired over a gas-bearing reservoir is suggestive that the approach generates potential indicators of both fluid presence and stress prediction.

INTRODUCTION

Hydraulic fracturing is a core technology in the development of unconventional (e.g., shale and tight sand) reservoirs. In the application of this technology, reliable methods for estimation of subsurface effective stress are sought, to guide selection of fracturing targets and to design drilling trajectories. Effective stress is related to vertical stress and pore pressure. So, one procedure to predict effective stress is to first estimate vertical stress and pore pressure separately, and then to calculate the effective stress using these as input. In this approach, the accuracy of the effective stress prediction is controlled by those of the vertical stress estimation and the pore pressure calculation. An alternative approach is to relate reservoir properties (e.g. porosity) to stress parameters. In the present study we adopt this second approach, setting up a workflow based on the relationship between porosity and effective stress (as set out by Athy, 1930; Zoback, 2010), from which seismic-derived elastic properties (bulk and shear moduli, P- and S-wave velocities, etc.) are connected to a stress-sensitive parameter.

Gassmann (1951) formulated a theory within which effective bulk and shear moduli for saturated rocks can be computed. In the model, the effective bulk modulus is related to mineral bulk modulus, porosity, dry rock bulk modulus and fluid bulk modulus. Krief et al. (1990) presented a nonlinear equation from which to calculate the bulk modulus of dry rock using the total porosity. Based on the critical porosity (CP) model of Nur et al. (1998), a linear relationship was then proposed to compute the bulk modulus of the dry rock using the total porosity and the critical porosity (Mavko et al., 2009). Combining the linear relationship between dry rock bulk modulus and porosity, and the relation between porosity and effective stress, our approach is to re-express the fluid substitution equation in terms of the dry rock bulk modulus and the effective stress-sensitive parameter.

In order to estimate this stress-sensitive parameter from observed seismic data, a reflection coefficient related to stress is required. We follow Shaw and Sen (2006), who presented a general formulation relating to leading order perturbations in the elastic stiffness matrix and reflection coefficients. After re-expressing the fluid substitution equation in terms of stress, we derive the stiffness matrix using the stress related bulk modulus of saturated rocks. We then express the perturbation in each stiffness parameter in the case of an interface separating two layers and, following Shaw and Sen, obtain a linearized P-to-P reflection coefficient as a function of stress-sensitive parameter. Based on this reflection coefficient expression, an elastic impedance (EI) can be straightforwardly formulated. This becomes the foundation for the nonlinear inversion algorithm.

Full waveform inversion (e.g., Virieux and Operto, 2009) is currently being developed as a tool for onshore reservoir characterization and monitoring. However, much existing technology for seismic characterization connected to relatively sophisticated rock physics is within an amplitude-variation-with-offset (AVO) and azimuth (AVAZ) framework (e.g., Chen et al., 2018b). The quantities and ideas within AVO inversion have been shown to be closely connected with those of FWI (Innanen, 2014). In this paper we do not formulate the inversion directly as an FWI optimization – in particular, the convolution-reflectivity wave model is retained. However, we do formulate the amplitude method with several features which emerge from the AVO-FWI analysis: we formulate an iterative, nonlinear inverse problem; we develop it in terms of gradients of a least-squares data misfit; and, we set up sensitivities based on an elastic scattering model. Transforming the approach further, such that it involves waveform fitting, is the subject of ongoing research.

THEORY AND METHOD

Elastic properties related to effective stress

Based on the fluid substitution model of Gassmann (1951), the saturated rock bulk modulus, K_{sat}, is given at low frequencies by (Mavko et al., 2009)

$$K_{\text{sat}} = K_{\text{dry}} + \frac{\left(1 - K_{\text{dry}}/K_0\right)^2}{\phi/K_{\text{f}} + (1-\phi)/K_0 - K_{\text{dry}}/K_0^2}, \qquad (1)$$

where ϕ is the porosity, K_{f} is the effective bulk modulus of filling fluid, and K_{dry} and K_0 are respectively the effective bulk moduli of dry rock and the minerals that make up the rock. Nur et al. (1998) proposed a critical porosity (CP) model, within which the relationship between the effective bulk modulus of dry rock, K_{dry}, and the porosity ϕ, is given by

$$K_{\mathrm{dry}} = K_0\left(1-\phi/\phi_{\mathrm{c}}\right), \tag{2}$$

where ϕ_{c} is the critical porosity, which separates the consolidated rock domain from the suspension domain. Substituting equation 2 into equation 1 yields

$$K_{\mathrm{sat}} = K_{\mathrm{dry}} + \frac{K_0\left(\phi/\phi_{\mathrm{c}}\right)^2}{\phi K_0/K_{\mathrm{f}} - \left(\phi - \frac{\phi}{\phi_{\mathrm{c}}}\right)}. \tag{3}$$

Because $K_0 \gg K_{\mathrm{f}}$, we assume $\phi K_0/K_{\mathrm{f}} \gg \left(\phi - \frac{\phi}{\phi_{\mathrm{c}}}\right)$, in which case equation 3 simplifies to

$$K_{\mathrm{sat}} \approx K_{\mathrm{dry}} + \phi/\phi_{\mathrm{c}}^2\, K_{\mathrm{f}}. \tag{4}$$

We next relate the effective bulk modulus of saturated rock K_{sat} to the effective stress σ_{e} felt by the rock, by involving a stress-dependent porosity $\phi(\sigma_{\mathrm{e}})$. Smith (1971) proposed a simple exponential porosity-effective stress function of the form

$$\phi \approx \phi_0 P_{\mathrm{e}}, \tag{5}$$

where P_{e} is related to effective stress by $P_{\mathrm{e}} = \exp\left(-a\sigma_{\mathrm{e}}\right)$, in which a is related to rock compaction, and ϕ_0 is the initial porosity, which is assumed to be equal to ϕ_{c} in the present study. Substituting equation 5 into equation 4, we obtain

$$K_{\mathrm{sat}} \approx K_{\mathrm{dry}} + K_{\mathrm{f}}/\phi_{\mathrm{c}}\, P_{\mathrm{e}}. \tag{6}$$

Based on Gassmann's model, we also assume the effective shear modulus of saturated rock to be equal to that of dry rock (i.e. $\mu = \mu_{\mathrm{sat}} = \mu_{\mathrm{dry}}$). The shear modulus μ is calculated by

$$\mu = \mu_0\left(1-\phi/\phi_{\mathrm{c}}\right), \tag{7}$$

where μ_0 is the effective shear modulus of minerals making up the rock. These values can then be used to model the effect of stress in the rock stiffness matrix

$$\mathrm{C} = \begin{bmatrix} C_{33} & C_{33}-2C_{55} & C_{33}-2C_{55} & 0 & 0 & 0 \\ C_{33}-2C_{55} & C_{33} & C_{33}-2C_{55} & 0 & 0 & 0 \\ C_{33}-2C_{55} & C_{33}-2C_{55} & C_{33} & 0 & 0 & 0 \\ 0 & 0 & 0 & C_{55} & 0 & 0 \\ 0 & 0 & 0 & 0 & C_{55} & 0 \\ 0 & 0 & 0 & 0 & 0 & C_{55} \end{bmatrix}, \tag{8}$$

where $C_{33} = K_{\mathrm{sat}} + \frac{4}{3}\mu$, and $C_{55} = \mu$.

Linearized PP-wave reflection coefficient

The relationship between the scattering function $\mathscr{S}$ and the P-to-P reflection coefficient R_{PP} is (Shaw and Sen, 2006)

$$R_{\mathrm{PP}} = \mathscr{S}/\left(4\rho\cos^2\theta\right), \tag{9}$$

where ρ is the reference density and θ is the P-wave incidence angle. The scattering function $\mathscr{S}$ is related to perturbations in density and stiffness parameters (Shaw and Sen, 2006). The perturbation ΔC_{33} is expressed as

$$\Delta C_{33} \approx \Delta K_{\mathrm{dry}} + P_{\mathrm{e}}/\phi_{\mathrm{c}}\Delta K_{\mathrm{f}} + K_{\mathrm{f}}/\phi_{\mathrm{c}}\Delta P_{\mathrm{e}}, \tag{10}$$

in which we have neglected the term proportional to $\Delta K_{\mathrm{f}}\Delta P_{\mathrm{e}}$ under the assumption of small changes in both the fluid bulk modulus and the stress parameter across the interface. The perturbation in C_{55} is expressed as

$$\Delta C_{55} = \Delta\mu. \tag{11}$$

Combining equations 9-11 a linearized expression for the P-to-P reflection coefficient is obtained

$$R_{\mathrm{PP}} = \frac{1}{2\cos^2\theta}\left(\frac{\gamma_{\mathrm{sat}}}{\gamma_{\mathrm{dry}}} - \frac{4}{3}\gamma_{\mathrm{sat}}\right)R_{K_{\mathrm{dry}}} - 4\gamma_{\mathrm{sat}}\sin^2\theta R_\mu + \frac{\cos 2\theta}{2\cos^2\theta}R_F + \frac{1}{2\cos^2\theta}\left(2\sin^2\theta - \frac{\gamma_{\mathrm{sat}}}{\gamma_{\mathrm{dry}}}\right)R_{K_{\mathrm{f}}} + \frac{1}{2\cos^2\theta}\left(1 - \frac{\gamma_{\mathrm{sat}}}{\gamma_{\mathrm{dry}}}\right)R_{P_{\mathrm{e}}}, \tag{12}$$

where

$$R_{K_{\mathrm{dry}}} = \frac{\Delta K_{\mathrm{dry}}}{2K_{\mathrm{dry}}},\ R_\mu = \frac{\Delta\mu}{2\mu},\ R_F = \frac{\Delta F}{2F},\ R_{K_{\mathrm{f}}} = \frac{\Delta K_{\mathrm{f}}}{2K_{\mathrm{f}}},\ R_{P_{\mathrm{e}}} = \frac{\Delta P_{\mathrm{e}}}{2P_{\mathrm{e}}}, \tag{13}$$

and where F is the fluid-sensitive factor $F = \rho K_{\mathrm{f}}$, γ_{sat} and γ_{dry} are moduli ratios of dry and saturated rocks.

Nonlinear inversion for dry rock, fluid, and stress parameters

In this section we formulate an inverse procedure with which to estimate the dry rock bulk modulus, fluid-sensitive factor and the stress-sensitive parameter. This involves the approximations:

$$R_{\mathrm{PP}} = \Delta\mathrm{EI}/(2\mathrm{EI}) \approx \Delta\ln(\mathrm{EI})/2, \tag{14}$$

and

$$\begin{aligned} &R_{K_{\mathrm{dry}}} \approx \frac{1}{2}\Delta\ln\left(K_{\mathrm{dry}}\right),\ R_\mu \approx \frac{1}{2}\Delta\ln(\mu), \\ &R_F \approx \frac{1}{2}\Delta\ln(F),\ R_{K_{\mathrm{f}}} \approx \frac{1}{2}\Delta\ln\left(K_{\mathrm{f}}\right), R_{P_{\mathrm{e}}} \approx \frac{1}{2}\Delta\ln\left(P_{\mathrm{e}}\right), \end{aligned} \tag{15}$$

where EI is the elastic impedance (Connolly, 1999; Whitcombe, 2002; Chen et al., 2018a). Making these substitutions in equation 12 leads to

$$\begin{aligned} \Delta\ln(\mathrm{EI}) = &\frac{1}{2\cos^2\theta}\left(\frac{\gamma_{\mathrm{sat}}}{\gamma_{\mathrm{dry}}} - \frac{4}{3}\gamma_{\mathrm{sat}}\right)\Delta\ln\left(K_{\mathrm{dry}}\right) \\ &- 4\gamma_{\mathrm{sat}}\sin^2\theta\Delta\ln(\mu) + \frac{\cos 2\theta}{2\cos^2\theta}\Delta\ln(F) \\ &+ \frac{1}{2\cos^2\theta}\left(2\sin^2\theta - \frac{\gamma_{\mathrm{sat}}}{\gamma_{\mathrm{dry}}}\right)\Delta\ln\left(K_{\mathrm{f}}\right) \\ &+ \frac{1}{2\cos^2\theta}\left(1 - \frac{\gamma_{\mathrm{sat}}}{\gamma_{\mathrm{dry}}}\right)\Delta\ln\left(P_{\mathrm{e}}\right). \end{aligned} \tag{16}$$

Integrating, we obtain

$$\mathrm{EI} = \mathrm{EI}_0\left[\left(\frac{K_{\mathrm{dry}}}{K_{\mathrm{dry0}}}\right)^{a_{K_{\mathrm{dry}}}(\theta)}\left(\frac{\mu}{\mu_0}\right)^{a_\mu(\theta)}\left(\frac{F}{F_0}\right)^{a_F(\theta)}\left(\frac{K_{\mathrm{f}}}{K_{\mathrm{f0}}}\right)^{a_{K_{\mathrm{f}}}(\theta)}\left(\frac{P_{\mathrm{e}}}{P_{\mathrm{e0}}}\right)^{a_{P_{\mathrm{e}}}(\theta)}\right], \tag{17}$$

where $a_{K_{\mathrm{dry}}}(\theta) = \frac{1}{2\cos^2\theta}\left(\frac{\gamma_{\mathrm{sat}}}{\gamma_{\mathrm{dry}}} - \frac{4}{3}\gamma_{\mathrm{sat}}\right)$, $a_\mu(\theta) = -4\gamma_{\mathrm{sat}}\sin^2\theta$, $a_F(\theta) = \frac{\cos 2\theta}{2\cos^2\theta}$, $a_{K_{\mathrm{f}}}(\theta) = \frac{1}{2\cos^2\theta}\left(2\sin^2\theta - \frac{\gamma_{\mathrm{sat}}}{\gamma_{\mathrm{dry}}}\right)$, $a_{P_{\mathrm{e}}}(\theta) =$

$\frac{1}{2\cos^2\theta}\left(1-\frac{\gamma_{sat}}{\gamma_{dry}}\right)$, and $\mathrm{EI}_0=\alpha_0\rho_0$. The α_0 and ρ_0 are are the constant background P-wave velocity and density, and these, along with the background K_{dry0}, μ_0, F_0, K_{f0} and P_{e0} are to be obtained from well log data (Whitcombe, 2002).

The forward modelling operator we use relates a vector of seismic amplitude data $\mathbf{s}$ and the corresponding EI for n horizontal interfaces:

$$\mathbf{s}(\theta_i)=\mathbf{WD}\,\mathbf{e}(\theta_i), \tag{18}$$

where

$$\mathbf{s}(\theta_i)=\begin{bmatrix} s_1\\ s_2\\ \vdots\\ s_n\end{bmatrix},\mathbf{W}=\begin{bmatrix} w_1 & 0 & \dots & 0\\ w_2 & w_1 & \dots & 0\\ \vdots & \vdots & \ddots & \vdots\\ w_n & w_{n-1} & \dots & w_1\end{bmatrix},$$

$$\mathbf{D}=\frac{1}{2}\begin{bmatrix} -1 & 1 & & & \\ & -1 & 1 & & \\ & & \ddots & \ddots & \\ & & & -1 & 1\end{bmatrix},\mathbf{e}(\theta_i)=\begin{bmatrix}\log(\mathrm{EI}_1)\\ \log(\mathrm{EI}_2)\\ \vdots\\ \log(\mathrm{EI}_{n+1})\end{bmatrix}, \tag{19}$$

in which the w_j are time samples of the source wavelet, the s_j are time samples of the input seismic data at incidence angle θ_i, $\mathbf{D}$ is an $n\times(n+1)$ differencing operator, and the $\log(\mathrm{EI}_j)$ are time samples of the logarithm of the elastic impedance EI at incidence angle θ_i. Using equation 18, we may estimate EI datasets from the observed seismic data stacked over different ranges of incidence angle, following the model-constrained least-squares algorithm introduced by Chen et al. (2018a).

We may then use these impedance values as input to a nonlinear inversion to determine the dry rock bulk modulus, fluid-sensitive factor and stress-sensitive parameter. A nonlinear relationship between EI and the unknown parameter vector in the case of six incidence angles (θ_1, θ_2, θ_3, θ_4, θ_5 and θ_6) and n reflection interface is given by

$$\mathbf{d}=\mathbf{G}(\mathbf{m}), \tag{20}$$

where

$$\mathbf{d}=\begin{bmatrix}\mathbf{EI}(\theta_1)\\ \mathbf{EI}(\theta_2)\\ \mathbf{EI}(\theta_3)\\ \mathbf{EI}(\theta_4)\\ \mathbf{EI}(\theta_5)\\ \mathbf{EI}(\theta_6)\end{bmatrix},\mathbf{m}=\begin{bmatrix}\mathbf{K}_{dry}\\ \mu\\ \mathbf{F}\\ \mathbf{K}_f\\ \mathbf{P}_e\end{bmatrix}, \tag{21}$$

and $\mathbf{G}$ is an operator containing the reflectivity weights in equation 12:

$$\mathbf{G}=\begin{bmatrix}\mathbf{a}_{K_{dry}}(\theta_1) & \mathbf{a}_{\mu}(\theta_1) & \mathbf{a}_F(\theta_1) & \mathbf{a}_{K_f}(\theta_1) & \mathbf{a}_{P_e}(\theta_1)\\ \vdots & \vdots & \vdots & \vdots & \vdots\\ \mathbf{a}_{K_{dry}}(\theta_6) & \mathbf{a}_{\mu}(\theta_6) & \mathbf{a}_F(\theta_6) & \mathbf{a}_{K_f}(\theta_6) & \mathbf{a}_{P_e}(\theta_6)\end{bmatrix}. \tag{22}$$

Let $\mathbf{d}_{obs}$ be the vector of EI determined from the input data; let $\mathbf{d}_{mod}$ be the simulated impedance data associated with a model $\mathbf{m}_{mod}$. The L2-norm of the misfit is given by

$$J=\|\mathbf{d}_{mod}-\mathbf{d}_{obs}\|_2=\frac{1}{2}(\delta\mathbf{d})^T(\delta\mathbf{d}), \tag{23}$$

where J represents the energy of the data residual, which is to be minimized. We update the model iteratively, i.e., $\mathbf{m}=\mathbf{m}_i+\delta\mathbf{m}$, where $\delta\mathbf{m}$ is a step based on an appropriate search direction for each iteration, and $\mathbf{m}_i$ is the current model. A full Newton step $\delta\mathbf{m}$ is $\delta\mathbf{m}=-\mathbf{H}^{-1}\mathbf{g}$, where $\mathbf{g}=\left(\frac{\partial J}{\partial\mathbf{m}}\right)$ is the gradient of J with respect to $\mathbf{m}$, and $\mathbf{H}$ is the Hessian matrix (e.g., Choi et al., 2008; Köhn, 2011). The gradient is

$$\begin{aligned}\frac{\partial J}{\partial\mathbf{m}}&=\frac{\partial\left[\frac{1}{2}(\mathbf{d}_{mod}-\mathbf{d}_{obs})^T(\mathbf{d}_{mod}-\mathbf{d}_{obs})\right]}{\partial\mathbf{m}}\\ &=\frac{\partial\mathbf{d}_{mod}(\mathbf{m})}{\partial\mathbf{m}}(\delta\mathbf{d}),\end{aligned} \tag{24}$$

in which the sensitivity of the synthetic EI data to $\mathbf{m}$, $\frac{\partial\mathbf{d}_{mod}(\mathbf{m})}{\partial\mathbf{m}}$, is given by

$$\frac{\partial\mathbf{d}_{mod}(\mathbf{m})}{\partial\mathbf{m}}=\left[\frac{\partial(\mathrm{EI})}{\partial(\mathbf{K}_{dry})}\ \frac{\partial(\mathrm{EI})}{\partial(\mu)}\ \frac{\partial(\mathrm{EI})}{\partial(\mathbf{F})}\ \frac{\partial(\mathrm{EI})}{\partial(\mathbf{K}_f)}\ \frac{\partial(\mathrm{EI})}{\partial(\mathbf{P}_e)}\right]^T, \tag{25}$$

assuming that the vectors of variables, $\mathbf{K}_{dry}$, μ, $\mathbf{F}$, $\mathbf{K}_f$ and $\mathbf{P}_e$, in the vector $\mathbf{m}$ are independent of each other.

SYNTHETIC EXAMPLES

Synthetic inversion results

We first utilize a well-log model to generate synthetic seismic data using the Zoeppritz equations, with random noise added, and then we examine the response of the proposed inversion approach. In Figure 1 we plot profiles of noisy seismic data, with signal-to-noise ratio (SNR) of 2, and incidence angle range $1^\circ-30^\circ$. The input for the first stage of the inversion, wherein EI is obtained, involves stacking the pre-stack seismic data over different ranges of incidence angle (i.e. $1^\circ-6^\circ$, $7^\circ-12^\circ$, $13^\circ-18^\circ$, $19^\circ-24^\circ$, and $25^\circ-30^\circ$). The incidence angles used in equation 22 are the centers of these ranges, namely $\theta_1=3^\circ$, $\theta_2=9^\circ$, $\theta_3=15^\circ$, $\theta_4=21^\circ$ and $\theta_5=27^\circ$.

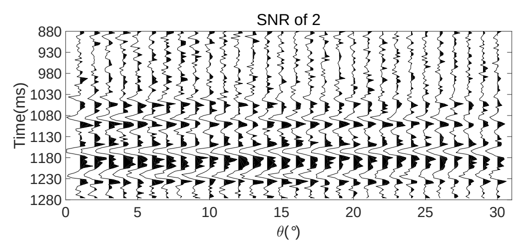

Figure 1: Profiles of noisy seismic data. The signal-to-noise ratio (SNR) is 2.

The EI are thus estimated; comparisons between these inversion results and values computed using equation 17 are plotted in Figure 2. We match is suggestive that EI values so derived can be used as input in the inversion for unknown parameters. We next apply the second stage of the inversion, determining unknown parameters K_{dry}, μ, F, K_f, and P_e. These step-wise outputs are plotted alongside and their corresponding true values in Figure 3. We again observe a match between derived and true properties which is suggestive of both the accuracy and stability (in the sense of random noise) of the approach.

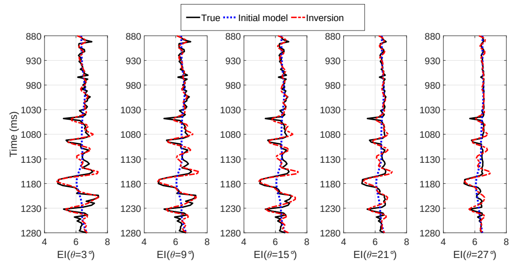

Figure 2: Comparisons between inversion results and true values of EI.

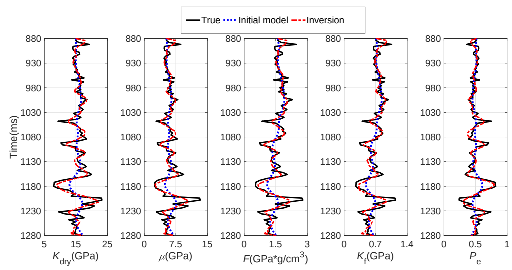

Figure 3: Comparisons between inversion results and true values.

FIELD DATA EXAMPLE

With evidence in place of the stability of the proposed approach in the presence of noisy synthetic data, we next test the inversion using a field data set acquired over a hydrocarbon reservoir. We employ stacked seismic data after standard AVO-compliant processing, with central angles ($\theta_1 = 3^\circ$, $\theta_2 = 9^\circ$, $\theta_3 = 15^\circ$, $\theta_4 = 21^\circ$ and $\theta_5 = 27^\circ$), to implement the estimation of EI data sets, as plotted in Figure 4. We observe that the EI exhibits relatively low values in the vicinity of the gas-bearing reservoir.

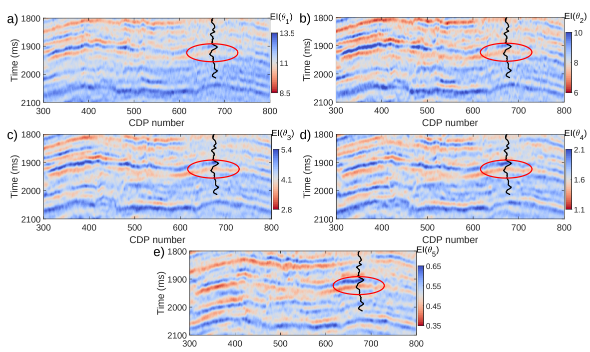

Figure 4: Inversion results of EI. The incidence angles are $\theta_1 = 3^\circ$, $\theta_2 = 9^\circ$, $\theta_3 = 15^\circ$, $\theta_4 = 21^\circ$ and $\theta_5 = 27^\circ$. The P-wave velocity log data are overlain (black).

With the inversion results of EI in hand, we proceed to the four-step nonlinear inversion for the bulk and shear moduli of dry rock, fluid-sensitive factor and bulk modulus of fluid, and stress-sensitive parameter. In Figure 5 the inverted K_{dry}, μ, F, K_{f} and P_{e} are plotted. The inverted bulk and shear moduli of

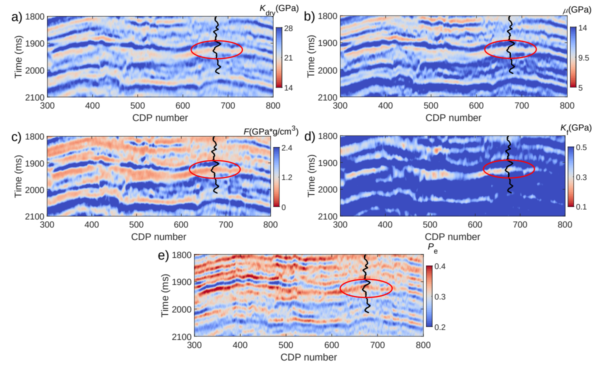

Figure 5: Inversion results. The P-wave velocity log data are overlain (black).

dry rock, fluid factor, bulk modulus of fluid and stress-sensitive parameter are consistent with the P-wave velocity well log data; we observe that the K_{dry}, μ, F and K_{f} models exhibit relatively low values in the vicinity of the reservoir (as marked by an ellipse in each figure); in the same area the estimated stress-sensitive parameter exhibits a relatively high value.

CONCLUSIONS

We obtain a simplified approximation of the fluid substitution equation, in which we introduce a stress-sensitive parameter based on the critical porosity model. Relating stiffness parameters to the stress-sensitive parameters, we express perturbations in stiffness parameters across an interface separating two layers. Using the perturbations, we derive a linearized reflection coefficient in terms of reflectivities of dry rock bulk modulus, shear modulus, fluid-sensitive factor, fluid bulk modulus and stress-sensitive parameter, and we also transfer the derived reflection coefficient to elastic impedance (EI). Based on the EI expressions, we establish a four-step nonlinear inversion approach to estimate dry rock elastic properties, fluid factor, and stress-sensitive parameter. The stability of the nonlinear inversion is verified using noisy synthetic seismic data generated using the full Zoeppritz equations. Applying the proposed inversion approach to real data that have undergone amplitude-preserving processing, we conclude that estimates of this kind may be capable of guiding rock-physics interpretation, specifically fluid identification and stress prediction.

ACKNOWLEDGMENTS

The industrial sponsors of CREWES are thanked for their support. We gratefully acknowledge additional support from the NSERC through the grant no. CRDPJ 461179-13. This research was undertaken thanks in part to funding from the CFREF, and the Mitacs Accelerate grant. The SINOPEC is thanked for providing the processed real data.